UDC 621.923 **doi: 10.20998/2078-7405.2023.99.12**

SURFACE TEMPERATURES AND VACATION BURNS OCCURRING DURING GRINDING OF CEMENTED GEARS WITH TWO DISHED WHEELS ON DIFFERENT PARTS OF THE MACHINED INVOLUTE PROFILE

Volodymyr **Tonkonogyi** [1][0000-0003-1459-9870], Oleksiy **Yakymov** [1][0000-0003-2096-4555], Liubov **Bovnegra** [1][0000-0003-0429-2816], Fedir **Novikov** [2][0000-0001-6996-3356]

[1]Odesa Polytechnic National University, 1, Schevchenko av., Odesa, 65044, Ukraine
[2]Simon Kuznets Kharkiv National University of Economics, 9-A Nauky Av., Kharkiv 61166, Ukraine
novikovfv@i.ua

Received: 09 November 2023 / Revised:16 November 2023 / Accepted: 25 November 2023 / Published: 01 December 2023

Abstract. *To increase grinding productivity with the provision of specified physical and mechanical properties of the surface layer of the surface layer of the processed part it is necessary to know the temperature on the surface of the workpiece, since its value depends on the depth of the defective surface layer. In the work theoretically justified the difference of surface temperatures in the initial (at the base), in the middle (on the dividing circle) and final (at the top) points of involute profile of the gear tooth when grinding with two disc wheels on the zero scheme. The difference in temperature at different points of the processed tooth profile is justified by the fact that at different parts of the trajectory of the movement of the heat source acts a different number of thermal pulses. These pulses have different duration and time intervals between the actions of these pulses in different points of the involute profile are also different. The number of thermal actions on a fixed point of the machined profile depends on the length of the heat source, and the duration of heating of the surface at this point is determined by the width of the heat source. The duration of cooling depends on the location of the point on the involute profile. Mathematical models have been developed to calculate the temperatures at different parts of the trajectory of the rolling path of a disc grinding wheel on the tooth being machined. Each of these formulas contains two sums. The first sum determines the temperature increase at a fixed point of the tooth profile under repeated exposure to thermal pulses during the forward stroke, and the second sum - during the reverse stroke. Mathematical models are based on the principle of superposition of thermal fields. It is found that the temperature in the middle part of the tooth is 40% less than at the tooth apex and 20% less than at the tooth base. The engineering method of distribution of the total allowance by passes at multi-pass gear grinding with two dished wheels according to the zero scheme has been developed. The method is based on the experimental dependence of the depth of the defect layer on the depth of cutting, which has a linear character. In the work, calculations were made on the allowance distribution in the initial, middle and final points of the involute tooth profile. The calculations showed that in order to prevent burns on the final machined surface, grinding in different parts of the machined profile should be performed with a different number of passes. The smallest number of passes on the separating circle, and the largest - on the top of the tooth. The proposed methodology of distribution of allowances by passes can be used at the stage of design of gear grinding operation (for optimization of modes) and at the stage of machining (for diagnostics of the*

operation). It is theoretically substantiated that calculations of allowance distribution by passes should be made only for the tooth head. To increase grinding productivity with provision of the specified physical and mechanical properties of the surface layer of the processed part it is necessary to know the temperature on the surface of the workpiece, as its value depends on the depth of the defective surface layer. In the work theoretically justified the difference in surface temperatures in the initial (at the base), in the middle (on the dividing circle) and final (at the top) points of involute profile of the gear tooth when grinding with two disk wheels on the zero scheme. The difference in temperature at different points of the processed tooth profile is justified by the fact that at different parts of the trajectory of the heat source acts a different number of thermal pulses. These pulses have different duration and time intervals between the actions of these pulses in different points of the involute profile are also different. The number of thermal actions on a fixed point of the machined profile depends on the length of the heat source, and the duration of heating of the surface at this point is determined by the width of the heat source. The duration of cooling depends on the location of the point on the involute profile. Mathematical models have been developed to calculate the temperatures at various parts of the rolling path of a dished grinding wheel on a machined tooth. Each of these formulas contains two sums.
Keywords: *dished wheels; zero scheme; tempering burns; multi-pass grinding.*

1. INTRODUCTION

The rapid development of mechatronics is not accompanied by a marked reduction in the need for gears. The continuous development of technology leads to increasingly stringent requirements for gears. The requirements for minimizing the weight and size of gears are coupled with the need to be able to operate at high speeds, transfer high loads and at the same time provide increased operational reliability and durability. To meet these requirements, gears must be manufactured to 3 - 4 degrees of accuracy, and the working surfaces of their teeth must have high hardness (HRC 60-62). Surface hardness of teeth is provided by chemical-thermal treatment, after which the gear ring warps. To eliminate errors caused by deformation of the teeth and warping of the crown and to ensure the required accuracy of manufacturing of gears is possible only by grinding. The grinding process is accompanied by thermal impact on the machined surface [1, 2], causing the appearance of burns (structural changes) and residual tensile stresses [3, 4], which reduce the durability of the gear wheel in terms of contact endurance by 3 - 5 times, and in terms of bending endurance by 1.4 - 1.6 times. In spite of this, gear grinding is still an indispensable method of finishing.

Gear grinding with two disc wheels allows to obtain gear wheels of 3-4 degrees of accuracy with surface roughness R_a = 1.0 - 0.3 mkm [5, 6]. At the zero method of grinding with two disc wheels the wheels are set parallel to each other at a distance equal to the length of the common normal) [7, 8]. The advantage of the "zero method" of gear grinding over the "15-degree method" is the absence of a "mesh" on the grinding surfaces of the teeth. The main disadvantage of the process of grinding with disc-shaped wheels according to the zero-degree scheme is high thermal stress. To predict the possibility of thermal defects, it is necessary to study the mechanism of heat generation during gear grinding. Modeling of thermal

processes occurring during grinding of involute tooth profiles is devoted to works [9 – 11]. The authors of [12, 13] studied the mechanism of heat generation during gear grinding. Gear grinding is characterized by periodically alternating stages of heating and cooling of each point of the machined surface. In [14], formulas for calculating the surface temperature at each of these stages were obtained. The structure of these formulas includes the requirement that at the moment of the end of the heating stage, the instantaneous temperature distribution is the initial condition for modeling the temperature field at the cooling stage. The formulas for temperature calculation proposed in [14] are valid only for profile gear grinding. The zero-point gear grinding scheme with two disc wheels is widely used in aircraft engine building and shipbuilding, despite the fact that the production of machines operating under this scheme has been discontinued due to their low productivity. It can be stated that abrasive high-precision hobbing is currently experiencing a crisis associated with the search for new effective methods, technologies and tools that increase its productivity [15 – 17].

Goal of the work – development of engineering methodology of allowance distribution at multi-pass grinding of cemented spur gears with two dished wheels according to the zero scheme, providing the given physical and mechanical characteristics of quality of surface layers of the final-machined teeth.

2. RESEARCH METHODOLOGY

Theoretical studies were carried out on the basis of scientific fundamentals of mechanical engineering technology, metal science, thermal physics of cutting. To investigate the quality of the surface layer of the working surfaces of gear wheels, their microhardness was measured, and the detection of burns was carried out by color defectoscopy. Cylindrical spur gears (m=2 mm; z=20) made of 12X2H4A steel (E3310X (USA), X12Ni5 (Germany), SNC815 (Japan), 13NiCr14 (France), 655N13 (England), 12Ch2N4A (Bulgaria), 12H2N4A (Poland), 16420 (Czech Republic)) were investigated. The heat treatment of the gears consisted of cementation in a solid carburetorizer at 900 ºC to a depth of 1.1÷ 1.3 mm, high tempering at 650 ºC, double hardening at 850 ± 20 ºC and at 800 ± 20 ºC, cold treatment in liquid nitrogen and tempering at 150 ± 10 ºC. The gears were machined on a Maag SS ½ X gear grinding machine with disk grinding wheels 24A F60 K 10 V5 using a zero scheme (Fig. 1).

The distribution of microhardness along the depth of the surface layer was determined on the PMT-3 device by the "oblique slices" method. The teeth-samples were obtained as follows. On a lathe with abundant cooling with emulsion, the toothed crown was separated from the hub. After cutting, the crown was broken into individual teeth. After burn etching, oblique flat cuts were made on the tooth

specimens at an angle of 2º30′ ± 10′ at the tooth base, near the dividing circle and at the tooth apex (Fig. 2 a, b, c, respectively).

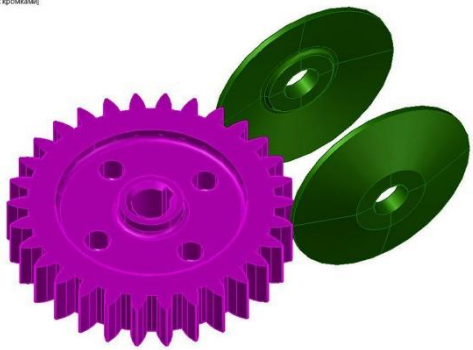

Figure 1 – Zero grinding method

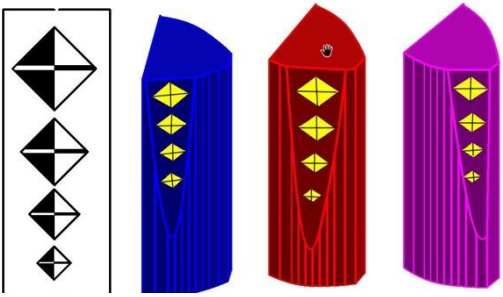

Figure 2 – Microhardness measurement locations on oblique sections made at the tooth base (a), in the area of the dividing circumference (b), on the tooth head (c) using the PMT-3 instrument

The roughness height of the flat slices corresponded to roughness class 13 R_z = 1.00 ÷ 0.05 mkm). Etching for burn-in detection was performed in four steps: 1) etching at room temperature in aqueous solution of ammonium sulfate (100 ÷ 150 g/l) for 15 ÷ 30 s followed by rinsing in cold water; 2) etching at room temperature in aqueous solution of hydrochloric acid (50 ÷ 100 g/l) for 60 s followed by rinsing in cold water; 3) neutralization at room temperature in aqueous solution of sodium carbonate (30 ÷ 50 g/l) for 1 ÷ 3 min; 4) anticorrosion treatment in aqueous solution of sodium nitrate (200 ÷ 250 g/l) for 1 ÷ 3 min.

The dark-etching zone is a tempering product, has an underestimated hardness compared to the base metal and is a ferrite-carbide mixture. Hardness was measured on a PMT-3 microhardness tester by pressing a diamond tip in the form of a regular tetrahedral pyramid with a dihedral angle at the apex of 136º at a load of 100 g into the surface of an oblique slice and measuring the linear quantity of

the diagonal of the resulting imprint. The hardness number was calculated by dividing the load by the surface area of the indentation, assuming that the angles of the indentation correspond to the angles of the pyramid. Microhardness measurements on oblique slices were made at four points equidistant from each other at equal distances of 50 mkm (Fig. 2).

3. RESEARCH RESULTS

A characteristic feature of the zero method of gear grinding is the different intensity of heat generation in different parts of the rolling path of the disc wheel along the involute profile of the tooth. The difference of temperatures formed on different fragments of the rolling trajectory is explained by the fact that different thermal processes occur in different points of the involute profile due to different amounts of thermal influences on these points, different time intervals between interactions, and different durations of influences. Fig. 3 shows three points of contact between the disk grinding wheel and the tooth being machined, one of which is located at the base of the tooth (Fig. 4), one near the dividing circle (Fig. 5), and one at the head of the tooth (Fig. 6). The dimensions of the contact patch of the disc wheel with the tooth of the wheel change continuously during the running-in process.

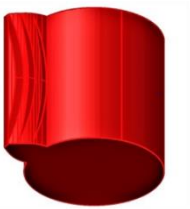

Figure 3 – Contact spots of the dished wheel with different parts of the involute tooth profile

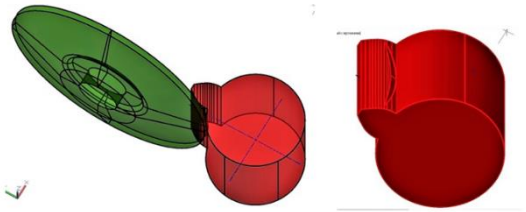

a b

Figure 4 – Contact area between the dished grinding wheel (a) and the lower part of the involute tooth profile (b)

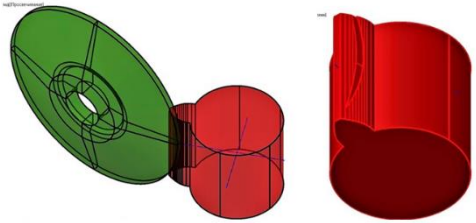

a b

Figure 5 – Contact area between the dished grinding wheel (a) and the involute tooth profile in the area of the dividing cylinder (b)

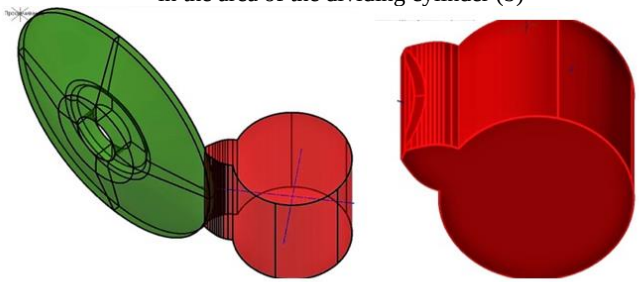

a b

Figure 6 – Contact spot between the dished grinding wheel (a) with the upper part of the involute tooth profile (b)

When running the abrasive tool over the tooth in the direction of the trough, the area of the spot decreases, and when running in the direction of the tooth apex, the area of the spot increases. This is due to the variability of the involute radius of curvature within the height of the machined tooth: it is the largest at the tooth apex and the smallest at the tooth base (Fig. 7, Fig. 8).

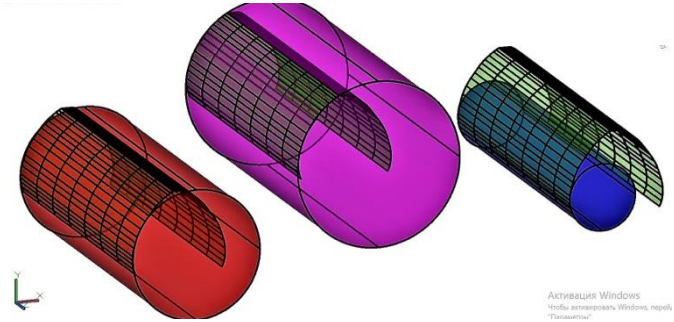

Figure 7 – Straight circular cylinders imitating fragments of involute tooth profile on the head, stem and middle part of the tooth.

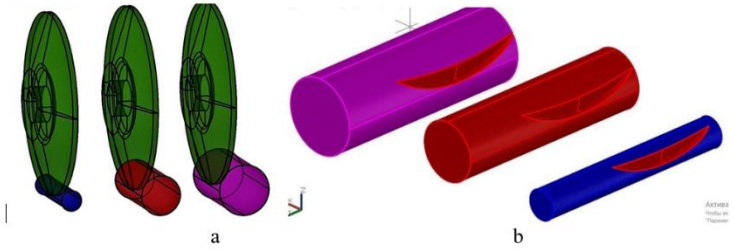

a b

Figure 8 – Contact spots of the dished grinding wheel (a) with cylinders simulating the involute tooth profile on the head (purple), stem (blue) and in the area of the dividing cylinder (red) (b)

In Fig. 9 – Fig. 11 show the actual shape of the contact spot of the dished grinding wheel with the tooth to be machined (its length is X).

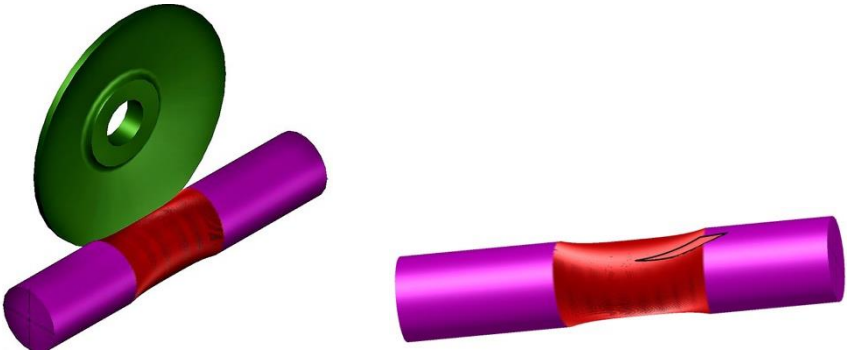

a b

Figure 9 – Actual contact patch of the dished wheel (a) with the cylinder simulating involute profile on the tooth head, taking into account the displacement of the tool from the previously machined area in the direction of the feed rate by the value of the running-in path (b).

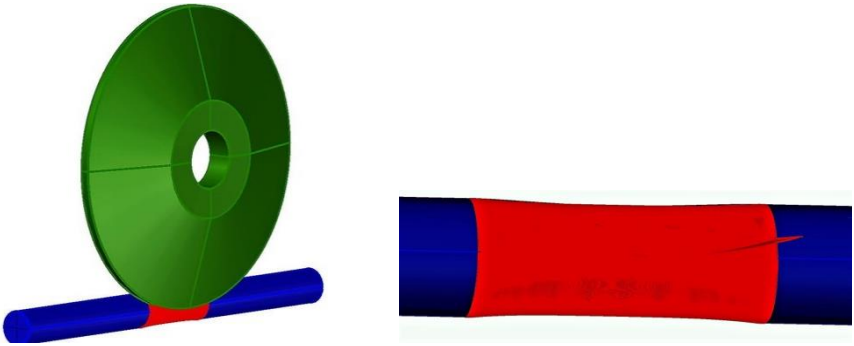

a b

Figure 10 – Actual contact patch of the dished wheel (a) with the involute cylinder at the tooth base, taking into account the pre-machined section of the gear width with subsequent tool displacement in the longitudinal feed direction (b).

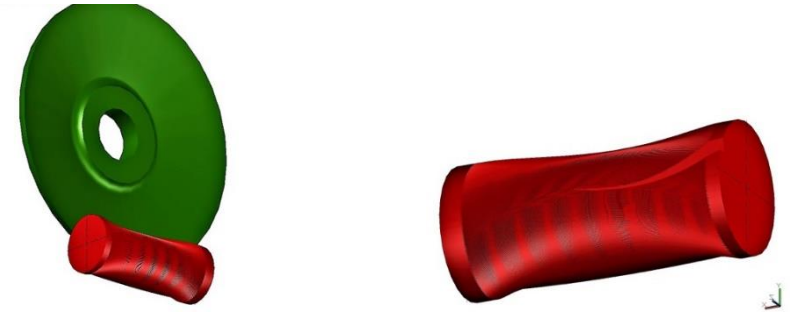

a b

Figure 11 – Actual contact patch of the dished wheel (a) with the cylinder simulating an involute profile in the area of the dividing circle, taking into account the displacement of the tool from the machined area in the working feed direction by an amount corresponding of the value to the running-in path (b).

Usually in technical literature, the contact spot is taken as a segment with maximum thickness in the center and length equal to 2X. This is due to the fact that when the wheel contacts the workpiece, the presence of a transition area (cutting zone) and a previously machined surface on the tooth is usually not taken into account. This leads to distortion of the shape and significant overestimation of the contact area. If the boundaries of the contact spot of the abrasive tool with the tooth of the gear are taken as the boundaries of the thermal source, the latter in the process of grinding the tooth on the zero scheme will repeatedly pass over each point of the machined surface and met with the areas of the heat conducting space, preheated on the previous running-in movements. The points located on different parts of the machined surface perceive different amounts of thermal influences: the point located on the tooth head experiences 7 heatings (Fig. 12, Fig. 13), the point on the dividing circle - 5 (Fig. 14, Fig. 15), and the point on the tooth base is heated 3 times (Fig. 16, Fig. 17). Within the tooth height, the probability of thermal defects has a variable character and in most cases takes the maximum values at its head [18, 19].

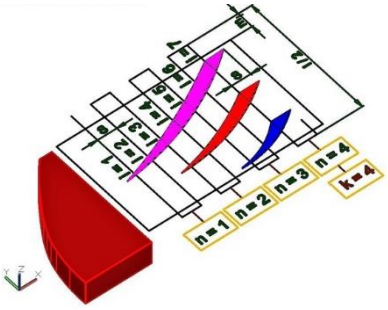

Figure 12 – Schematic of the point under the heat source during four double break-in movements of the dished wheel on the tooth being machined when the heat source is located on the tooth head.

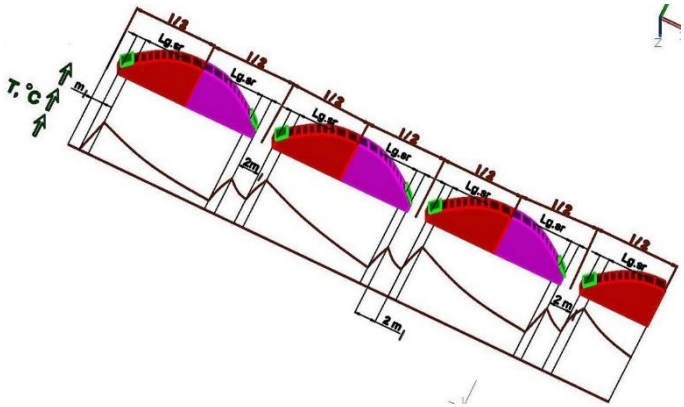

Figure 13 – Change of surface temperature at the point located on the tooth head for the total time of four double break-in movements of the dished wheel on the machined involute profile

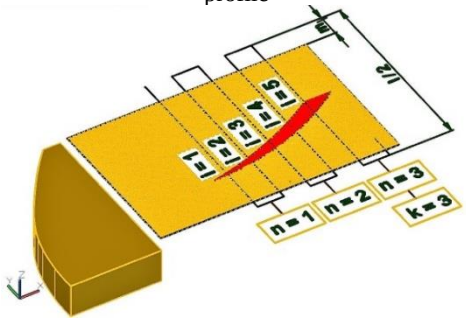

Figure 14 – Schematic of passing the point under the heat source for the time of three double break-in movements of the dished wheel on the tooth when the heat source is located on the dividing circle

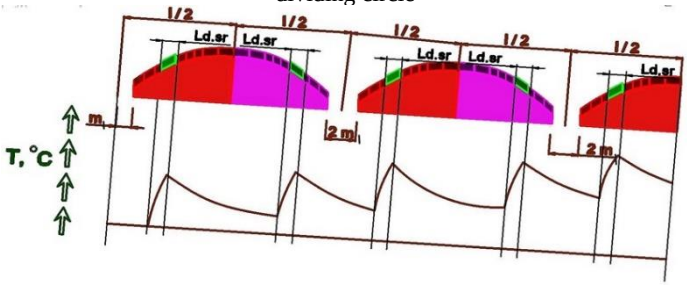

Figure 15 – Change of surface temperature at the point located in the crop circle area for the total time of three double break-in movements of the dished wheel on the machined involute profile

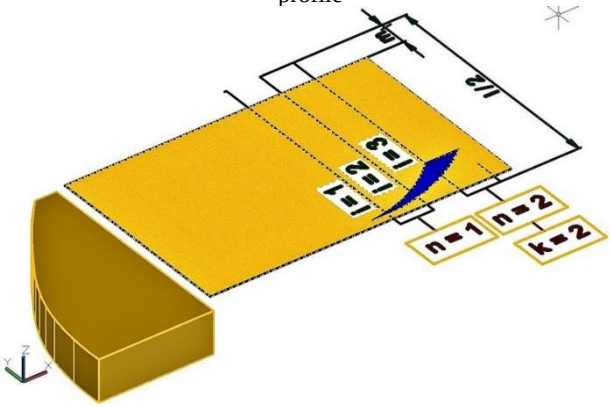

Figure 16 – Schematic of the point under the heat source for the time of two double break-in movements of the dished wheel on the tooth when the heat source is located near the tooth base.

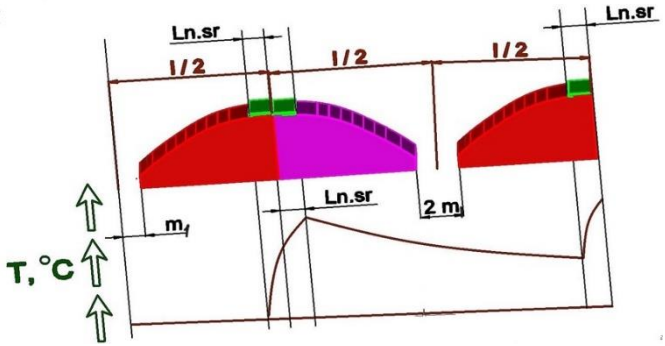

Figure 17 – Variation of surface temperature at a point located at the tooth base for the total time of two double break-in movements of a dished wheel along an involute profile.

For theoretical substantiation of localization of thermal defects on the tooth head it is necessary to be able to make calculations of temperatures on different parts of tooth side surfaces, arising during grinding with disc-shaped wheels according to the zero-pass scheme, taking into account repeated heat exposure on each point of the machined surface. As a basis for modeling the temperature fields in multi-pass grinding, we will use a one-dimensional thermophysical scheme in which a point of the heat conducting medium is subjected to repeated heating. Fig. 13 shows the scheme of a point passing under a fixed planar heat source of width L_g.sr located near the tooth apex. The following

designations are adopted in the scheme: *l*/2 - length of forward or reverse break-in movements, numerically equal to the sum of the tooth height and the value of the abrasive tool exit beyond the machined tooth m_1:

$$l/2 = m + 1{,}25m + m_1,$$

where *m* is the modulus of the gear wheel; *l* is the length of the full break-in movements, equal to the sum of the lengths of the forward and reverse strokes.

On Fig. 13 shows the heating scheme of a point as it passes 7 times under a planar heat source located near the tooth apex.

From Fig. 12 and Fig. 13, it can be seen that the number of point passes under the heat source depends on its length *X* and the magnitude of the longitudinal feed *S*.

The number of heated points increases with increasing contact patch size and with decreasing longitudinal feed. The duration of heated point increases with increasing width of the heat source L_g.sr:

$$L_g.sr = \frac{1}{2\cdot k}\cdot \sum_{i=1}^{2\cdot k} L_g \cdot i; \tag{1}$$

$$L_g.i = \sqrt{2\cdot r\cdot t_i - t_i^2} \quad \text{for } 1 \le i \le 2\cdot k; \tag{2}$$

where *r* is the radius of curvature of the edge of the dished grinding wheel; $r = 0.4\cdot m$; t_i - thicknesses of layers removed by the abrasive tool during one break-in movements in different parts of the contact patch:

$$t_1 = \left(\rho_g + r\right) - \Delta_1; \tag{3}$$

ρ_g – radius of curvature of the involute at the tooth head;

$$t_i = \left(\rho_{g.i-1} + r\right) - \Delta_1 \quad \text{for } 2 \le i \le 2\cdot k; \tag{4}$$

$$\Delta_i = \sqrt{\left(\rho_{g.i-1} - t_i + r\right)^2 + \theta_i^2} \quad \text{for } 1 \le i \le 2\cdot k; \tag{5}$$

$$\rho_{g.i} = \rho_g - \sum_{i=1}^{2\cdot k} t_i; \tag{6}$$

$$\theta_i = \frac{2\cdot\left(R_{kr} - r\right) - \sqrt{\left[2\cdot\left(R_{kr} - r\right)\right]^2 - 4\cdot\left(X_g - i\cdot S\right)^2}}{2}; \tag{7}$$

R_{kr} is the radius of the grinding wheel; X_g – length of the contact spot of the circle with the tooth on the head:

$$X_g = \sqrt{2 \cdot \rho_g \cdot t_0 - t_0^2}; \quad (8)$$

t_0 - cutting depth;

$$2 \cdot k = \frac{X_g - S}{S}. \quad (9)$$

On Fig. 13 shows the pattern of temperature rise in a single point of the machined surface as it moves under a flat stationary heat source located on the head of the tooth being machined.

The formula for calculating temperatures, which takes into account the multiplicity of thermal effects on a separately taken point of the lateral surface of the tooth when the heat source is located near the apex of the tooth, is as follows:

$$T_k = \frac{2 \cdot \psi \cdot q_g}{\sqrt{c \cdot \rho_m \cdot \lambda}} \cdot \sum_{n=1}^{k} \left[\sqrt{\frac{(k-n) \cdot I - 2m_1}{V_{obk}}} \cdot ierfc\left(\frac{t_0}{2 \cdot \sqrt{a} \cdot \frac{(k-n) \cdot I + I - 2m_1}{V_{obk}}} \right) - \right.$$

$$\left. - \sqrt{\frac{(k-n) \cdot I + I - 2m_1 - L_g.sr}{V_{obk}}} \cdot ierfc\left(\frac{t_0}{2 \cdot \sqrt{a} \cdot \sqrt{\frac{(k-n) \cdot I + I - 2m_1 - L_g.sr}{V_{obk}}}} \right) \right] +$$

$$+ \frac{2 \cdot \psi \cdot q_g}{\sqrt{c \cdot \rho_m \cdot \lambda}} \cdot \sum_{n=1}^{k} \left[\sqrt{\frac{(k-n) \cdot I + L_g.sr}{V_{obk}}} \cdot ierfc\left(\frac{t_0}{2 \cdot \sqrt{a} \cdot \sqrt{\frac{(k-n) \cdot I + L_g.sr}{V_{obk}}}} \right) - \right.$$

$$\left. - \sqrt{\frac{(k-n) \cdot I}{V_{obk}}} \cdot ierfc\left(\frac{t_0}{2 \cdot \sqrt{a} \cdot \sqrt{\frac{(k-n) \cdot I}{V_{obk}}}} \right) \right], \quad (10)$$

where $a = \lambda / \left(c \cdot \rho_m \right)$ – thermal conductivity of the material to be processed, m^2/S; ψ – coefficient showing how much of the work is converted to heat; ρ_m, c, λ –density (kg/m^3), heat capacity ($I / \left(kg \cdot {}^oC \right)$ and thermal conductivity $I / \left(m \cdot S \cdot {}^oC \right)$ of the material to be processed respectively; q_g – heat flux density formed on the tooth head, W/m^2; V_{obk} – run-in speed, m/s;

$$V_{obk} = \frac{2 \cdot n'}{1000} \cdot tg \left(arccos \frac{r_\omega \cdot \cos \alpha_{t\omega}}{r_\omega + 1{,}2 \cdot m \cdot m_1} \right) \cdot R_p ; \quad (11)$$

n' – number of double rolling movements per minute; R_p – radius of the pitch circle of the machined wheel;

$$r_\omega = R_p = \frac{r_0}{\cos 20^o} = \frac{m \cdot z_1}{2} ; \quad (12)$$

z_1 – number of teeth on the machined wheel; m – wheel module; m_1 – the value of grinding wheel out of the tooth head when break-in movements; r_0 – radius of the main circumference of the wheel; $\alpha_{t\omega}$ – angle pressure.

Formula (10) contains two sums, one of which forms the temperature increase at a fixed point of the surface under the heat source during the crimping movements in the direction of the tooth-space, and the second sum provides the temperature increase during the break-in movements to the side of the apex of the tooth.

On Fig. 14 and Fig. 15 show one-dimensional thermophysical schemes, which are the basis for modeling the temperature field. In these schemes, a point of the heat conducting medium is subjected to multiple heating due to its multiple passages under a flat heat source of wide $L_d.sr$ located in the region of the dividing circumference. Fig. 15 illustrates the nature of the temperature field in the region of the dividing circumference formed during multi-pass gear grinding with a dished grinding wheel using the zero method. The formula for calculating the temperatures based on Fig. 14 and Fig. 15 is as follows:

$$T_k = \frac{2 \cdot \psi \cdot q_d}{\sqrt{c \cdot \rho_m \cdot \lambda}} \times$$

$$\times \sum_{n=1}^{k}\left[\sqrt{\frac{(k-n)\cdot l + L_d.sr}{V_{obk}} + \frac{l}{2\cdot V_{obk}}}\cdot ierfc\left(\frac{t_0}{2\cdot\sqrt{a}\cdot\sqrt{\frac{(k-n)\cdot l + L_d.sr}{V_{obk}} + \frac{l}{2\cdot V_{obk}}}}\right) - \right.$$

$$\left. - \sqrt{\frac{(k-n)\cdot l}{V_{obk}} + \frac{l}{2\cdot V_{obk}}}\cdot ierfc\left(\frac{t_0}{2\cdot\sqrt{a}\cdot\sqrt{\frac{(k-n)\cdot l}{V_{obk}} + \frac{l}{2\cdot V_{obk}}}}\right)\right] +$$

$$+ \frac{2\cdot\psi\cdot q_d}{\sqrt{c\cdot\rho_m\cdot\lambda}}\cdot\sum_{n=1}^{k}\left[\sqrt{\frac{(k-n)\cdot l + L_d.sr}{V_{obk}} + \frac{l}{2\cdot V_{obk}}}\cdot ierfc\left(\frac{t_0}{2\cdot\sqrt{a}\cdot\sqrt{\frac{(k-n)\cdot l + L_d.sr}{V_{obk}}}}\right) - \right.$$

$$\left. - \sqrt{\frac{(k-n)\cdot l}{V_{obk}}}\cdot ierfc\left(\frac{t_0}{2\cdot\sqrt{a}\cdot\sqrt{\frac{(k-n)\cdot l}{V_{obk}}}}\right)\right]. \qquad (13)$$

Schemes of formation of temperature increases in the point moving along the trajectory of break-in movements of the dished grinding wheel on the tooth of the processed wheel and periodically passing under a fixed flat heat source, located near the base of the tooth, are shown in Fig. 16 and Fig. 17. Fig. 17 illustrates the nature of temperature change at this point in the process of grinding the tooth. The formula for calculating the temperatures based on Fig. 16 and Fig. 17 is as follows:

$$T_k = \frac{2\cdot\psi\cdot q_d}{\sqrt{c\cdot\rho_m\cdot\lambda}}\times$$

$$\times \sum_{n=1}^{k}\left[\sqrt{\frac{(k-n)\cdot l + 2L_n.sr}{V_{obk}}}\cdot ierfc\left(\frac{t_0}{2\cdot\sqrt{a}\cdot\frac{(k-n)\cdot l + 2L_n.sr}{V_{obk}}}\right) - \right.$$

$$-\sqrt{\frac{(k-n)\cdot l + L_n.sr}{V_{obk}}}\cdot ierfc\left(\frac{t_0}{2\cdot\sqrt{a}\cdot\sqrt{\frac{(k-n)\cdot l + L_n.sr}{V_{obk}}}}\right)\Bigg] +$$

$$+\frac{2\cdot\psi\cdot q_d}{\sqrt{c\cdot\rho_m\cdot\lambda}}\cdot\sum_{n=1}^{k}\Bigg[\sqrt{\frac{(k-n)\cdot l + L_n.sr}{V_{obk}}}\cdot ierfc\left(\frac{t_0}{2\cdot\sqrt{a}\cdot\sqrt{\frac{(k-n)\cdot l + L_n.sr}{V_{obk}}}}\right) -$$

$$-\sqrt{\frac{(k-n)\cdot l}{V_{obk}}}\cdot ierfc\left(\frac{t_0}{2\cdot\sqrt{a}\cdot\sqrt{\frac{(k-n)\cdot l}{V_{obk}}}}\right)\Bigg]. \qquad (14)$$

The Fig. 18 – Fig. 20 show the results of calculations of the lengths of the contact spots X of the processed gear, the number of passes of the point under the heat source $2\cdot k$ and temperatures T in points 1 (in the upper part of the tooth head), 2 (in the area of the dividing circumference) and 3 (in the area of the tooth base) at grinding of gears ($z = 20$, $m = 2$ mm, $m = 8$ mm) from cemented steel 18X2H4MA with a dished wheel mm on the zero pattern at modes: $t_0 = 0.05$ mm; $n' = 112$ min^{-1}; $S = 1.5$ mm; $S = 3$ mm.

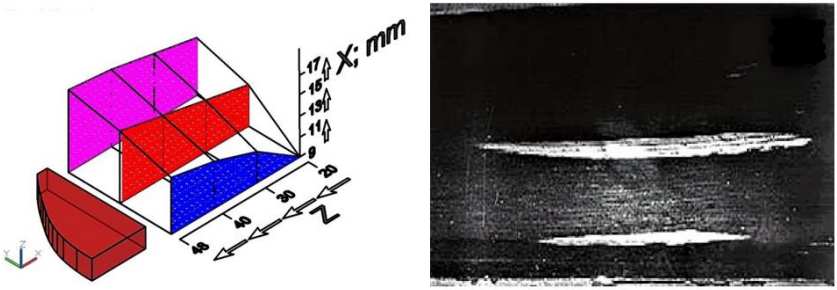

a b

Figure 18 – Increase in the length of the contact patch of a dished wheel with a gear tooth as it moves from the tooth base to its head for modulus *m*=2 mm and tooth counts 20< *z* <48: (a) calculated data; (b) experimental data [18]

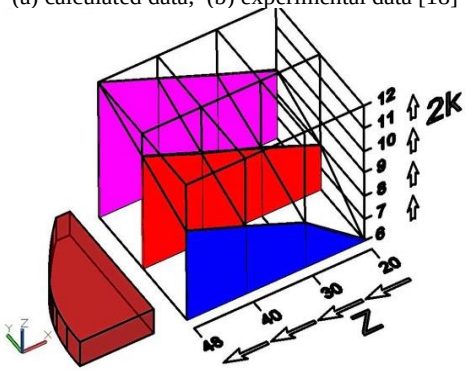

Figure 19 – Increase in the number of passes *2k* of the heat source over a fixed point of the machined surface at displacement of this point from the tooth base to its head for module *m*=2 mm and tooth counts 20< *z* <48

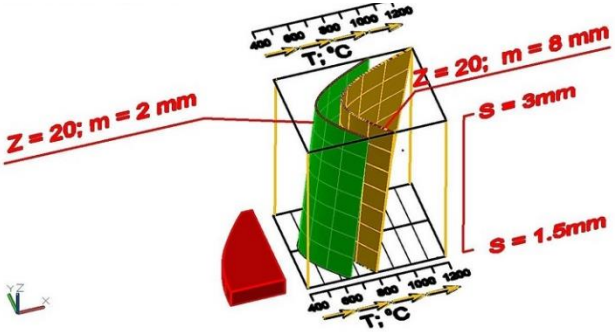

Figure 20 – Calculated temperatures formed during grinding of gear wheels (*z*=20; *m*=2 mm; *m*=8 mm) from cemented steel 18X2H4MA with a dished wheel according to the zero scheme on modes: *t*=0.05 mm; *n*`=112 1/min;
1.5 mm < *S* < 3.0 mm

The experimental determination of the contact area of a dished wheel with an involute tooth profile involved putting the tool into engagement with the wheel and measuring the resulting trace [18]. In this case, the contact area did not take into account the presence of a transition area (cutting zone) and a previously machined surface on the tooth being machined. In order to take into account these features of the shaping process, the gear wheel was pre-machined to a part of the width of its tooth crown corresponding to the studied phase of meshing of the tool with the wheel, then the tool was taken out of meshing and shifted in the direction

of longitudinal feed by the value of the break-in movements path. The grinding wheel left a trace on the tooth to be machined (Fig. 18, b).

Fig. 12 shows that in the process of break-in movements of the dished wheel in the direction of the tooth apex there is an increase in the length of the contact spot of the abrasive tool with the machined material.

In multi-pass grinding, the point at the base of the tooth absorbs fewer thermal influences than the point at the head. As the number of teeth increases, the number of contacts between the grinding wheel working surface and the fixed point of the involute profile being machined increases. Fig. 20 shows that the temperature in the middle part of the tooth profile is 35 % to 45 % less than at the head and 18 % to 22 % less than at the stem.

From Fig. 20, it can be seen that as the modulus m and longitudinal feed *S* increase, an increase in temperature *T* is observed.

At gear grinding with dished wheels, the dependence of the depth of the defective (tempered) layer h_d on the cutting depth *t* has a linear character (Fig. 21) [20].

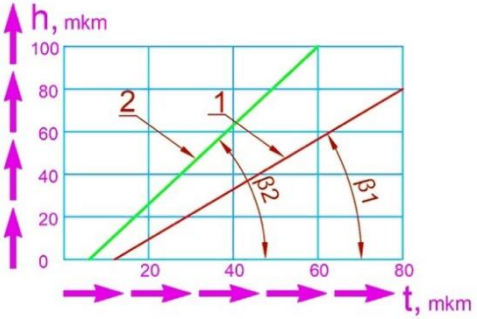

Figure 21 – Dependence of the depth of the defect layer on the grinding depth on machines operating with two dished wheels according to the "zero" (straight line 1) and "15-degree" (straight line 2) schemes.

Figure 22 –15- and 20-degree grinding method.

The graphs show that at the 15-degree grinding scheme (Fig. 22), temper burns begin to form at shallower cutting depths, and the process of propagation of critical temperatures deep into the workpiece proceeds more intensively compared to the "zero" scheme (Fig. 1). If the depths of the tempered layers $h_{d.a}$ and $h_{d.b}$ formed with cutting depths ta and t_b are determined experimentally, it is possible to determine the angle tangent of the line $tg\beta$, which defines the graph $h_d=f(t)$ (Fig. 23). The cutting depth t_0, at which no vacation burns, can be determined from the relations: $tg\beta = h\boldsymbol{d.b}\,/(t\boldsymbol{b} - t_0)$; $t_0 = (t\boldsymbol{b} \times tg\beta - h\boldsymbol{d.b})\,/\,tg\beta$.

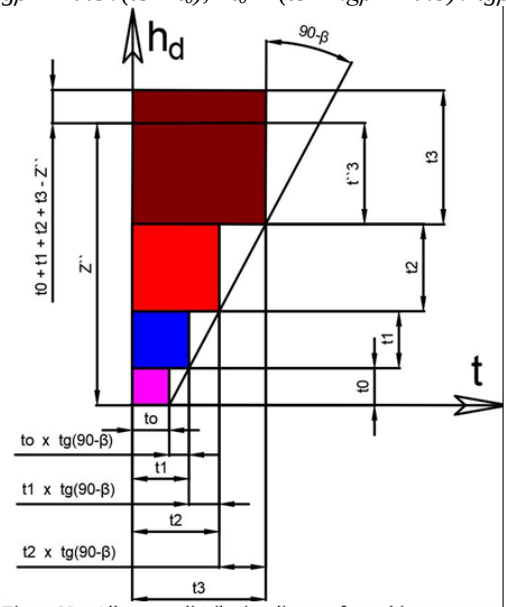

Figure 23 – Allowance distribution diagram for multi-pass gear grinding

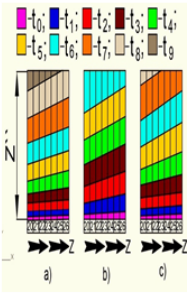

Figure 24 – Allowance distribution $z^{//}$ by passes calculated at the apex (a), on the dividing circle (b), and at the tooth base (c) for the tooth number range $20 < z < 26$ and constant modulus m=2 mm

Knowing the cutting depth t_0, at which no vacation burns are formed, and the angle β, it is possible to calculate the cutting depths for multi-pass grinding that satisfy the condition: the depth of burn propagation must not exceed the allowance remaining for subsequent passes. The depth of cut at different grinding passes is calculated by the formula: $\boldsymbol{ti} = ti\text{-}1 + \boldsymbol{ti\text{-}1} \times \mathrm{tg}(90^{o} - \beta)$, $i \geq 1$.

The numbering of the cutting depths at different grinding passes in Fig. 23 corresponds to the sequence of their calculation and does not coincide with the order of layer-by-layer removal of the allowance $z^{//}$. The sum of calculated cutting

depths t_i must be equal to the value of the total allowance $z^{//}$. If the sum of cut thicknesses of the machined material exceeds the allowance $z^{///}$, the last calculated depth of cut t_3 must be corrected downward $t_3^{///}$ (Fig. 23).

Fig. 24 shows the distribution of the total allowance $z^{//}$ by passes. Fig. 24 shows that different sections of the involute tooth profile require different numbers of grinding passes to prevent the appearance of temper burns: 10 - at the tooth apex (a), 7 - at the dividing circle (b), 9 - on the tooth base (c). The calculations of cutting depths t_i were carried out according to the method given in [20]. The obtained results can be explained by the fact that according to the graph (Fig. 20) the lowest heat stress in the area of the dividing circumference, so grinding can be carried out with greater cutting depths and, consequently, with a smaller number of passes. The highest heat stress is at the tooth apex, so more passes will be required to prevent vacation burns. Burns result in sharp hardness variations along the depth of the structurally altered layer. The greater the depth of penetration of the critical temperature deep into the part, the greater the reduction in microhardness at the surface. The higher the heat stress of grinding, the more intense the martensite tempering and the deeper the vacation burn. In order to reduce the depths of distribution of the vacation burn, it is necessary to reduce the depths of cutting when distributing the total allowance over grinding passes, and this leads to an increase in the number of technological transitions and, as a consequence, to an increase in the processing time and the cost of production of gears.

4. CONCLUSIONS

1. A mathematical model has been developed that allows calculations of surface temperatures during grinding of gear wheels with two dished wheels on a zero scheme.

2. Calculations have established that the temperatures and depths of penetration of critical temperatures, causing structural changes in the processed material, deep into the workpiece at different points of the trajectory of the grinding circumference break-in movements over the tooth are different: the farther from the dividing circle, the higher the grinding temperature and the thicker the depth of the defective layer.

3. The engineering methodology for determining the depths of cut at multi-pass grinding on the machines operating two dished wheels on the zero pattern is developed.

References: 1. *Ryabchenko S.V., Silchenko Ya.L., Fedorenko V.T., Polonsky L.G., Yanovsky V.A.* Quality analysis of surfacemachined with CBN disks. Machining in Mechanical Engineering: Transactions. Zhitomir: ZhSTU, 2015. Issue 15. 167-177. **2.** *Ren Xiao Zhong, Hu Hai Feng*. Analysis on the Temperature Field of Gear Form Grinding. Innovative Solutions in Materials Science and Engineering, 01 Sep 2014, Vol. 633-634,

Issue 2, pages 809-812. DOI: 10.4028/www.scientific.net/AMM.633-634.809 URL: http://www.scientific.net/AMM.633-634.809 **3.** *Jin T, Yi J, Peng S.* Determination of burn thresholds of precision gears in form grinding based on complex thermal modeling and Barkhausen noise measurements. Int J Adv Manuf Technol. 2017. 88(1-4). 789-800. **4.** *Guerrini G., Lerra F., Fortunato A.* The Effect of Radial Infeed on Surface Integrity in Dry Generating Gear Grinding for Industrial Production of Automotive Transmission Gears. J. Manuf. Process. 2019. 45. 234-241. Doi: 10.1016/j.jmapro.2019.07.006 **5.** *Larshin, V., Babiychuk, O., Lysyi, O., Uminsky, S.* Discontinuous Generating Gear Grinding Optimization. Lecture Notes in Mechanical Engineering, 2022, LNME, pp. 263-272, 2022. https://doi.org/10.1007/978-3-031-06025-0_26 https://www.scopus.com/authid/detail.uri?authorId=57217107788 **6.** *Ryabchenko S. V.* COG-WHEEL GRINDING WITH ABRASIVE CUBIC BORON NITRIDE DISKS. Vestnik Bryanskogo gosudarstvennogo tekhnicheskogo universiteta. 2018. №11(72). pp. 67–72. DOI:10.30987/article_5be14a35530b65.64215370 **7.** *Ryabchenko S.V., Polonskiy L.G., Golovnya V.D., Yanovskiy V.A., Kozyar Ya.A.* Shlifovaniye zubchatykh kolos krugami iz kubicheskogo nitrida bora. Vísnik ZHDTU. Seríya: Tekhníchní nauki 2017. No 2(80). pp. 68–72. DOI: https://doi.org/10.26642/tn-2017-2(80)-68-72 http://nbuv.gov.ua/UJRN/Vzhdtu_2017_2%281%29_13 **8.** *Sokolova I.D., Svitka A.S.* Analiz metodov shlifovaniya zubchatykh kolos na sovremennom oborudovanii. Innovatsionnaya nauka. Mezhdunarodnyy nauchnyy zhurnal. 2016. №9. pp. 83–87. [in Russian] **9.** *Shuying Yang, Weifang Chen, Su Nong, Lei Dong, Houyun Yu*. Temperature field modeling in the form grinding of involute gear based on high-order function moving heat source. Journal of Manufacturing Processes. Volume 81, September 2022. 1028–1039. https://doi.org/10.1016/j.jmapro.2022.07.014 **10.** *Jun Yi, Tan Jin, Wei Zhou, Zhaohui Deng*. Theoretical and experimental analysis of temperature distribution during full tooth groove form grinding. Journal of Manufacturing Processes, Volume 58, October 2022. pp. 101–115. https://doi.org/10.1016/j.jmapro.2020.08.011 **11.** *Jin Tan, Yi Jun, Li Ping*. Temperature distributions in form grinding of involute gears. Int J Adv Manuf Technol. 2017 (88). 2609–2620. **12.** *Lishchenko, N.* Profile gear grinding temperature determination. Transactions of Kremenchuk Mykhailo Ostrohradskyi National University. 2018. 100–108. https://doi.org/10.30929/1995-0519.2018.1.100-108 **13**. *Su J., Ke Q., Deng X. et al.* Numerical simulation and experimental analysis of temperature field of gear form grinding. Int J Adv Manuf Technol. 2018. 97. 2351–2367. https://doi.org/10.1007/s00170-018-2079-6 **14.** *Lishchenko N.V., Larshin V.P.* Profile Gear Grinding Temperature Reduction and Equalization. Journal of Engineering Sciences, Volume 5, Issue 1 (2018). A1-A7 DOI: 10.21272/jes.2018.5(1).a1 **15.** *Guerrini G., Landi E., Peiffer K., Fortunato A.* Dry Grinding for Sustainable Automotive Transmission Production. J. Clean. Prod. 2018. 176. 76–88. Doi: 10.1016/j.jclepro.2017.12.127. **16.** *Pashchenko E.O., Kukharenko S.A., Riabchenko S.V., Bychykhin V.M., Shatokhin V.V.* Development of the Technology for Manufacturing and Introducing a New Class of Tools with CVD-Diamond for Grinding High-Precision Gear Wheels of Special Reducer Units. Sci. Innov. 2020. V.16, No 1. https://doi.org/10.15407/scin16.01.069. **17.** *Riabchenko S., Lavrinenko V., Sheiko M., Paschenko E.* Elaboration of technology tor making the European nomenclature high-porous abrasive wheels of monocrystalline corund using a precision instrument of superhard materials for turbo-building of Ukraine Science and Innovation: Academic and Research Journal. Kyiv: National Academy of Sciences of Ukraine. 2018, volume 14(5). 49–56. **18.** *Ryabchenko S.V.* Shlifovaniye zubchatykh kolos tarel'chatymi krugami. Oborudovaniye i instrument dlya professionalov : mezhdunarodnyy informatsionno-tekhnicheskiy zhurnal (seriya: Metalloobrabotka). Khar'kov: Informatsionno-izdatel'skiy dom «Tsentr Inform». 2014. No 2. 44–48. [in Russian] **19**. *Jin T, Yi J* (2016) Investigation on the grinding force, power and heat flux distributions along the tooth profile in form grinding of gears. In: Proceedings of the ASME 2016 international manufacturing science and engineering conference MSEC2016, 27 June – 1 July 2016, Blacksburg, Virginia, USA. **20.** *Novikov F. V., Zhovtobryukh V. A., Gusarev V. S., Naddachin V. B., Yakimov A. A., Andilakhay A. A., Sergeyev A. S., Novikov D. F.* Innovatsionnoye razvitiye sovremennykh tekhnologiy : monografiya. – Dnepr: LIRA. 2021. 280 p. [in Russian].

Володимир Тонконогий, Олексій Якимов, Любов Бовнегра, Одеса, Україна
Федір Новіков, Харків, Україна

ПОВЕРХНЕВІ ТЕМПЕРАТУРИ І ПРИПІКАННЯ ВІДПУСТКИ, ВИНИКАЮЧІ ПІД ЧАС ШЛІФУВАННЯ ЦЕМЕНТУЮЧИХ ЗУБЧАТИХ КОЛІС ДВОМА ТАРІЛЬЧАСТИМИ КРУГАМИ, НА РІЗНИХ ДІЛЯНКАХ ОБРОБЛЮВАНОГО ЕВОЛЬВЕНТНОГО ПРОФІЛЮ

Анотація. *Для підвищення продуктивності шліфування із забезпеченням заданих фізико-механічних властивостей поверхневого шару оброблюваної деталі необхідно знати температуру на поверхні заготовки, оскільки від її величини залежить глибина дефектного поверхневого шару. У роботі теоретично обґрунтовано відмінність поверхневих температур у початковій (біля основи), у середній (на ділильному колі) і кінцевій (біля вершини) точках евольвентного профілю зуба шестірні при шліфуванні двома тарілчастими кругами за нульовою схемою. Відмінність температур у різних точках оброблюваного профілю обґрунтовується тим, що на різних ділянках траєкторії переміщення теплового джерела діє різна кількість теплових імпульсів. Ці імпульси мають різну тривалість та проміжки часу між діями цих імпульсів у різних точках евольвентного профілю теж різні. Кількість теплових дій на фіксовану точку оброблюваного профілю залежить від довжини теплового джерела, а тривалість нагрівання поверхні в цій точці визначається шириною теплового джерела. Тривалість охолодження залежить від місця розташування точки на евольвентному профілі. Розроблено математичні моделі для розрахунку температур на різних ділянках траєкторії обкатування тарілчастого шліфувального круга по оброблюваному зубу. Кожна з цих формул містить дві суми. Перша сума визначає збільшення температури у фіксованій точці профілю зуба при багаторазовій дії на неї теплових імпульсів при прямих ходах, а друга сума – при зворотних ходах. Математичні моделі ґрунтуються на принципі суперпозиції теплових полів. Встановлено, що температура в середній частині зуба на 40% менше, ніж у вершини зуба і на 20% менше, ніж у його основи. Розроблено інженерну методику розподілу загального припуску за проходами для багатопрохідного зубошліфування двома тарілчастими кругами за нульовою схемою. Методика ґрунтується на експериментальній залежності глибини дефектного шару від глибини різання, що має лінійний характер. У роботі виконано розрахунки з розподілу припуску в початковій, середній та кінцевій точках евольвентного профілю зуба. Розрахунки показали, що для запобігання появі припікань на остаточно-обробленій поверхні шліфування на різних ділянках оброблюваного профілю повинно здійснюватися з різним числом проходів. Найменша кількість проходів на ділильному колі, а найбільша – біля вершини зуба. Запропонована методика розподілу припуску за проходами може бути використана на етапі проектування операції зубошліфування (для оптимізації режимів) і на етапі механічної обробки (при діагностиці операції). Теоретично обґрунтовано, що розрахунки з розподілу припуску за проходами слід здійснювати тільки на головці зуба.*

Ключові слова: *тарілчасті круги; нульова схема; припікання відпалу; багатопрохідне шліфування.*